



## THE INFLUENCE OF NEAR-FAULT MOTIONS ON LIQUEFACTION TRIGGERING DURING THE CANTERBURY EARTHQUAKE SEQUENCE

Lake CARTER<sup>1</sup>, Russell GREEN<sup>2</sup>, Brendon BRADLEY<sup>3</sup>, and Misko CUBRINOVSKI<sup>4</sup>

### ABSTRACT

The objective of this study is to examine the influence of near-fault motions on liquefaction triggering in Christchurch and neighboring towns during the 2010-2011 Canterbury earthquake sequence (CES). The CES began with the 4 September 2010,  $M_w$  7.1 Darfield earthquake and included up to ten events that triggered liquefaction. However, most notably, widespread liquefaction was induced by the Darfield earthquake and the  $M_w$  6.2, 22 February 2011 Christchurch earthquake. Of particular relevance to this study is the forward directivity effects that were prevalent in the motions recorded during the Darfield earthquake, and to a much lesser extent, during the Christchurch earthquake. A 2D variant of the Richart-Newmark fatigue theory was used to compute the equivalent number of cycles ( $n_{eq}$ ) for the ground motions, where volumetric strain was used as the damage metric. This study is unique because it considers the contribution and phasing of both the fault-normal and fault-parallel components of motion on  $n_{eq}$  and the magnitude scaling factor (MSF). It was found that when the fault-normal and fault-parallel motions were treated individually, the former yielded a lower  $n_{eq}$  than the latter. Additionally, when the combined effects of fault-normal and fault-parallel components were considered, it was found that the MSF were higher than those commonly used. This implies that motions containing near-fault effects are less demanding on the soil than motions that do not. This may be one of several factors that resulted in less severe liquefaction occurring during the Darfield earthquake than the Christchurch earthquake.

Keywords: Canterbury Earthquake Sequence, Liquefaction, Near-fault, Rupture Directivity

### INTRODUCTION

The objective of the study presented herein is to examine the influence, if any, of near-fault ground motion effects on liquefaction triggering in Christchurch, New Zealand, and neighboring towns during the 2010-2011 Canterbury earthquake sequence (CES). The Christchurch area experienced widespread liquefaction as a result of the CES. However, of the 10 events in the CES that are known to have caused liquefaction, the 4 September 2010,  $M_w$  7.1 Darfield and 22 February 2011,  $M_w$  6.2 Christchurch earthquakes were the most significant (Figure 1). Of particular relevance to this study is the forward directivity effects, a near-fault phenomenon, that were prevalent in the ground motions recorded during the Darfield earthquake, and to a much lesser extent, during the Christchurch earthquake (e.g., Bradley and Cubrinovski, 2011; Bradley, 2012a,b; Shahi and Baker, 2012). Forward

---

<sup>1</sup> Graduate Research Assistant, Department of Civil and Environmental Engineering, Virginia Tech, Blacksburg, Virginia, USA

<sup>2</sup> Professor, Department of Civil and Environmental Engineering, Virginia Tech, Blacksburg, Virginia, USA, E-Mail: rugreen@vt.edu

<sup>3</sup> Senior Lecturer, Department of Civil and Natural Resources Engineering, University of Canterbury, Christchurch, NZ

<sup>4</sup> Professor, Department of Civil and Natural Resources Engineering, University of Canterbury, Christchurch, NZ

directivity is a Doppler-type phenomenon resulting from the approximate equality of the fault rupture and shear wave velocities and can result in a double-sided velocity pulse in the fault-normal component of motion. The strike slip rupture mechanism of the Darfield earthquake and the orientation of the causative fault relative to Christchurch resulted in forward directivity effects to manifest throughout much of the city. In contrast, the predominantly reverse rupture mechanism of the Christchurch earthquake and the causative fault orientation only resulted in forward directivity effects in areas south of the city along the Port Hills. Several studies have examined the detrimental effects of near-fault motions on building structures (e.g., Hall et al., 1995; Alavi and Krawinkler, 2001; and Luco and Cornell, 2007), but relatively little attention has been given to near-fault effects on liquefaction, hence the objective of this study.

The present study differs from previous ones that examined the influence of directivity on liquefaction triggering (e.g., Green et al., 2008) because it considers the contribution and phasing of both the fault-normal and fault-parallel components of motion on the equivalent number of uniform cycles ( $n_{eq}$ ) and corresponding magnitude scaling factors (MSF). Towards this end, a variant of the macro cumulative damage fatigue theory proposed by Richart and Newmark (1948) (i.e., R-N fatigue theory) was used to compute  $n_{eq}$  for the earthquake motions, wherein volumetric strain was used as the damage metric. The R-N fatigue theory was extended to two-dimensional (2D) motions using numerical element tests, where the response of a finite element subjected to the 2D motions was defined by the reduced-order bounding-surface hypoplasticity constitutive model proposed by Li et al. (1992). The constitutive model was calibrated using published seismic compression data from strain-controlled cyclic simple shear tests performed on dry sand samples (Stewart et al., 2004; Duku et al., 2008).

In total, ten sets of fault-normal and fault-parallel components of near-fault motions recorded on rock ( $V_{S30} > 600$  m/s) were selected, with one of the sets being recorded during the CES. These motions were used as rock outcrop input motions in equivalent linear site response analyses, and shear strain time histories were computed at a reference depth that is approximately the modal depth to the center of the critical layers determined from the liquefaction case history database. These strain time histories were the motions used in conjunction with the R-N fatigue theory discussed above to compute  $n_{eq}$ . The resulting  $n_{eq}$  values were then used to compute near-fault MSF, which were compared with those used in simplified liquefaction evaluations (i.e., Youd et al., 2001) and do not account for near-fault effects.

In the following, an overview of the selection of ground motions and site response analyses is presented, followed by an outline of the 2D variant of the R-N fatigue theory used to compute the  $n_{eq}$  for the near-fault and reference  $M_w 7.5$  motions. Finally, trends in the computed  $n_{eq}$  and MSF for the near-fault motions are discussed and compared to the conventional relationships for  $n_{eq}$  and MSF.

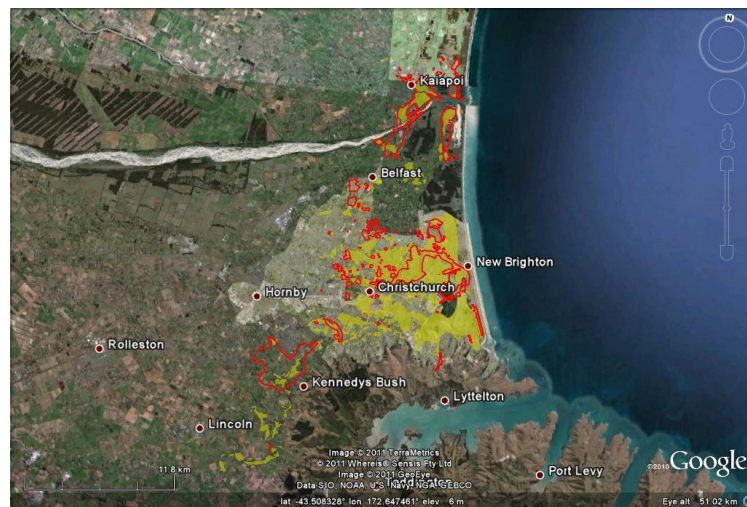


**Figure 1. Aerial image of Christchurch and neighboring towns. The areas bounded in red liquefied during the 4 September 2010,  $M_w 7.1$  Darfield earthquake and the areas highlighted in yellow liquefied during the 22 February 2011,  $M_w 6.2$  Christchurch earthquake.**

## SELECTION OF “NEAR-FAULT” MOTIONS

As stated above, ten sets of fault-normal and fault-parallel near-fault rock motions ( $V_{S30} > 600$  m/s) were used in this study; Table 1 lists the selected near-fault motions. Nine of the ten motions were taken from the NGA 1 database and one from a collection of near-fault CES motions (NGA Sequence number 6928). Other near-fault motions recording during the CES were not used in this study because the site conditions of the recording stations were other than rock. All the selected motion sets are considered to have forward directivity effects, manifested as “pulse-like” behavior in the fault-normal component, identified by Shahi and Baker (2012), and no observable velocity pulse in the fault-parallel component, consistent with the forward directivity phenomenon.

**Table 1. Near-Fault Motions**

NGA Sequence No.	Event	Year	Station	$M_w$	Distance* (km)
77	San Fernando	1971	Pacoima Dam (upper left abut)	6.61	1.81
150	Coyote Lake	1979	Gilroy Array #6	5.74	3.11
459	Morgan Hill	1984	Gilroy Array #6	6.19	9.86
828	Cape Mendocino	1992	Petrolia	7.01	8.18
879	Landers	1992	Lucerne	7.28	2.19
1013	Northridge - 01	1994	LA Dam	6.69	5.92
1051	Northridge – 01	1994	Pacoima Dam (upper left)	6.69	7.01
1511	Chi-Chi, Taiwan	1999	TCU076	7.62	2.76
1529	Chi-Chi, Taiwan	1999	TCU102	7.62	1.51
6928	Darfield, New Zealand	2010	LPCC	7.10	22.4

\*Closest distance to ruptured area on fault

## SITE RESPONSE ANALYSES

A series of site response analyses were performed using the selected sets of “near-fault” motions listed in Table 1. The motions were input as rock outcrop motions to the shear wave velocity profile shown in Figure 2, and shear strain time histories were computed at a reference depth,  $z_{ref}$ , of 4 meters. As shown in Figure 2, the profile assumes a constant soil unit weight of  $18.9 \text{ kN/m}^3$  ( $\approx 120 \text{ pcf}$ ), a ground water table depth of 1.5 meters, and shear wave velocities,  $V_s$ , that increase exponentially with depth given by the following equation:

$$V_s(z) = (V_s)_{z_{ref}} \left( \frac{z}{z_{ref}} \right)^{0.15} \quad (1)$$

where:  $(V_s)_{z_{ref}}$  is the shear wave velocity at the reference depth ( $z_{ref}$ ) of 4 m; and  $z$  is depth from the ground surface in the same units as  $z_{ref}$ ; and the power of 0.15 is typical for sand profiles (e.g., Lee, 2009).  $(V_s)_{z_{ref}}$  was estimated using the correlation proposed Andrus et al. (2004):

$$(V_s)_{z_{ref}} = 87.8 \cdot N_{1,60}^{0.253} \left( \frac{P_a}{\sigma'_v} \right)^{-0.25} \quad (2)$$

where:  $(V_s)_{z_{ref}}$  is in m/s;  $N_{1,60}$  is the Standard Penetration Test (SPT) blow count normalized/corrected to 1 atm of vertical effective confining stress and 60% hammer energy efficiency;  $P_a$  is atmospheric pressure; and  $\sigma'_v$  is the vertical effective stress at  $z_{ref}$  in the same units as  $P_a$ . In using Eqn 2,  $N_{1,60}$  was assumed to be 12 blows/0.3 m (or 12 blows/ft), which is approximately the modal blow count for the liquefaction case histories listed in Cetin’s (2000) database, consistent with assuming  $z_{ref} = 4$  m, which is approximately the modal depth to the center of the critical layers in Cetin’s (2000) liquefaction case history database.

As stated above, shear strain time histories were computed at a depth of 4 m (i.e.,  $z_{ref}$ ) for both fault-normal and fault-parallel components of motion. As outlined in the next section, these time histories were then used in conjunction with the R-N fatigue theory to compute  $n_{eq}$ .

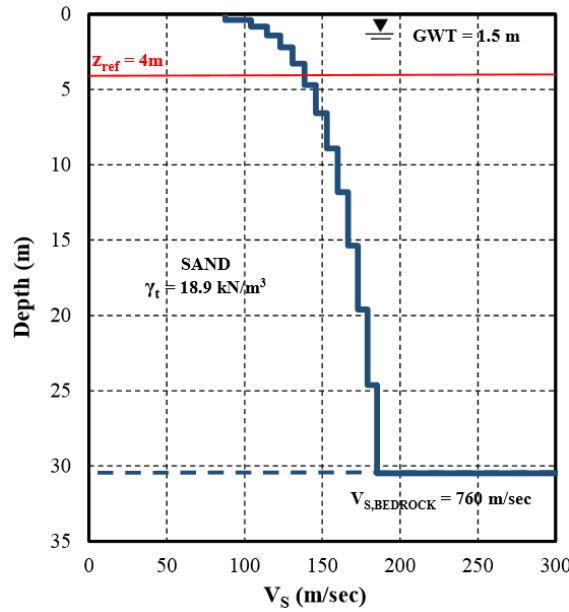


**Figure 2. Shear wave velocity profile used in the site response analyses**

### EQUIVALENT NUMBER OF UNIFORM CYCLES

The concept of converting a random load to an equivalently damaging number of sinusoidal cycles has its roots in metal fatigue theory. One of the earliest approaches was proposed by Palmgren (1924) and further developed by Miner (1945), with the approach commonly referred to as the Palmgren-Miner (P-M) fatigue theory. In the late 1960's to early 1970's, Professor H.B. Seed and colleagues adopted Miner's implementation procedure for the P-M theory, with slight modifications, to compute  $n_{eq}$  for evaluating the liquefaction triggering in soil (e.g., Seed et al., 1975a and Annaki and Lee, 1977). The Seed et al. variant of the P-M theory is still commonly used in geotechnical earthquake engineering studies today (e.g., Liu et al., 2001). However, several significant shortcomings of this procedure have been identified by Green and Terri (2005) and Green and Lee (2006), among others. Namely, the P-M theory, as adopted by Seed et al., applies to high cycle fatigue, which is characterized by a large number of load cycles (thousands to millions) wherein the material being loaded remains in the elastic range. As a corollary, the Seed et al. variant of the P-M theory fails to account for the absolute amplitude and sequencing of peaks in earthquake-induced ground motions, both of which are known to significantly influence excess pore pressure generation in saturated sands subjected to cyclic motions (Martin et al., 1975; Ishihara and Yasuda, 1973; Ishihara and Nagase, 1988).

As a result of the above limitations of the P-M theory, Green and Lee (2006) proposed the use of the R-N fatigue theory (Richart and Newmark, 1948) for computing  $n_{eq}$  for evaluating seismic compression in dry and partially saturated sands. The R-N theory can be applied to high and low cycle fatigue analyses, where the latter is characterized by a few load cycles (one to hundreds) and plastic deformations in the material being loaded (consistent with earthquake induced liquefaction). Furthermore, the R-N theory can account for both the absolute amplitude and sequencing of peaks in earthquake ground motions. As outlined in Green and Lee (2006), the Martin et al. (1975) procedure, and the Byrne (1991) simplified variant thereof, for computing volumetric strains in freely draining soils subjected to earthquake motions is an alternative form of the R-N fatigue theory. It is the Byrne (1991) formulation of the R-N theory that was adopted in this study, wherein volumetric strain is used as the damage metric to compute  $n_{eq}$  for strain time histories obtained from the site response analyses.

### Volumetric Strain Model & Equivalent Number of Cycles – One-directional Loading

The incremental volumetric strain induced in freely draining soil by each peak (or half cycle) in a shear strain time history is computed, per Byrne (1991), using the following relation:

$$(\Delta\varepsilon_v)_i = 0.5(|\gamma_i| - \gamma_{thresh})C_1 \exp\left(-C_2 \cdot \frac{(\varepsilon_v)_i}{(|\gamma_i| - \gamma_{thresh})}\right) \quad (3)$$

where  $(\Delta\varepsilon_v)_i$  is the incremental volumetric strain induced by the  $i^{\text{th}}$  peak in the shear strain time history;  $\gamma_i$  is the amplitude of the  $i^{\text{th}}$  peak in the shear strain time history;  $\gamma_{thresh}$  is the threshold shear strain below which no volumetric strain will occur (taken as 0.01% in this study);  $(\varepsilon_v)_i$  is the cumulative volumetric strain before the  $i^{\text{th}}$  peak in the shear strain time history is applied; and  $C_1$  and  $C_2$  are the material parameters. Assuming  $(\varepsilon_v)_i = 0$  for  $i = 1$ , the cumulative volumetric strain is incrementally computed by summing the incremental volumetric strain induced by successive peaks in the shear strain time history from the beginning to the end (i.e., for  $i = 1$  to  $n$ , where  $n$  is the total number of peaks in the shear strain time history):

$$(\varepsilon_v)_{i+1} = (\varepsilon_v)_i + (\Delta\varepsilon_v)_i \quad (4)$$

Byrne (1991) proposed the following generic relations for  $C_1$  and  $C_2$  for sands:

$$C_1 = 7600 \cdot D_r^{-2.5} \quad (5a)$$

$$C_2 = \frac{0.4}{c_1} \quad (5b)$$

where  $D_r$  is the relative density of the soil in percent.

The Byrne model is used to compute  $n_{eq}$  for a random load by equating the cumulative volumetric strains induced by the random load to that induced by  $n_{eq}$  of a sinusoidal load. In geotechnical engineering applications, the amplitude of the sinusoidal load is traditionally set equal to 0.65 times the absolute value of the maximum amplitude pulse in the earthquake motion (e.g., Seed et al., 1975a). Inherent to the above approach is the assumption that volumetric strain in dry sand is a valid damage metric for computing  $n_{eq}$  for use in liquefaction evaluations. At first glance, excess pore pressure ratio ( $r_u$ ) would be a seemingly more applicable damage metric for computing  $n_{eq}$  for liquefaction evaluations. However, a limitation of  $r_u$  is that it has the potential to reach a limiting value (i.e.,  $r_u = 1$ ) prior to the end of shaking, beyond which point subsequent motions do not contribute to the computed  $n_{eq}$ . As a result, several investigators have scaled the amplitude of the ground motions so that  $r_u = 1$  at the end of shaking (e.g., Ishihara and Nagase, 1988; Wer-Asturias, 1982). However, as mentioned previously, the absolute amplitude of the pulses in a ground motion are known to influence the liquefaction response of soil (e.g., Ishihara and Yasuda, 1974), and as a result, scaling of the ground motion amplitude is not desirable. Using the volumetric strain of dry sand as the damage metric avoids the ground motion scaling issue, and as discussed in Martin et al. (1975) and Byrne (1991) relates to excess pore pressure response in saturated sands.

#### Model Calibration

Although Byrne (1991) provides generic relations for estimating the material parameters  $C_1$  and  $C_2$  (i.e., Eqn 5), for this study,  $C_1$  was determined using published seismic compression data from strain-controlled cyclic simple shear tests performed on dry sand (Stewart et al., 2004). Eqn 5b was then used to determine  $C_2$ . Specifically,  $C_1$  was calibrated to the volumetric strains induced in dry Silica #2 sand samples having  $D_r = 45\%$  and subjected to 15 cycles of loading, for a range of shear strain amplitudes. However, the data from Stewart et al (2004) were based on tests conducted having an effective overburden pressure of 1 atm ( $\sim 101.3$  kPa), which differs from the vertical effective stress ( $\sigma'_{v,z_{ref}}$ ) at the reference depth used in this study (i.e.,  $z_{ref}$ ; Figure 2). Accordingly, before  $C_1$  was determined, the volumetric strains from Stewart et al. (2004) were adjusted to  $\sigma'_{v,z_{ref}}$  by applying the overburden correction factor ( $K_{\sigma,e}$ ) proposed by Duku et al. (2008):

$$K_{\sigma,\varepsilon} = \left( \frac{\sigma'_{v,z_{ref}}}{p_a} \right)^{-0.29} \quad (6)$$

$$(\varepsilon_v)_{\sigma'_{v,z_{ref}}} = (\varepsilon_v)_{1atm} \cdot K_{\sigma,\varepsilon} \quad (7)$$

where:  $(\varepsilon_v)_{\sigma'_{v,z_{ref}}}$  is volumetric strain corrected to  $\sigma'_{v,z_{ref}}$ , and  $(\varepsilon_v)_{1atm}$  is the volumetric strain obtained from the cyclic simple shear tests performed using a vertical effective confining stress of 1 atm.  $C_1$  was determined to be 0.51 and  $C_2$  was computed to be 0.78. Figure 3 shows a comparison between the Byrne model predictions and  $(\varepsilon_v)_{\sigma'_{v,z_{ref}}}$ .

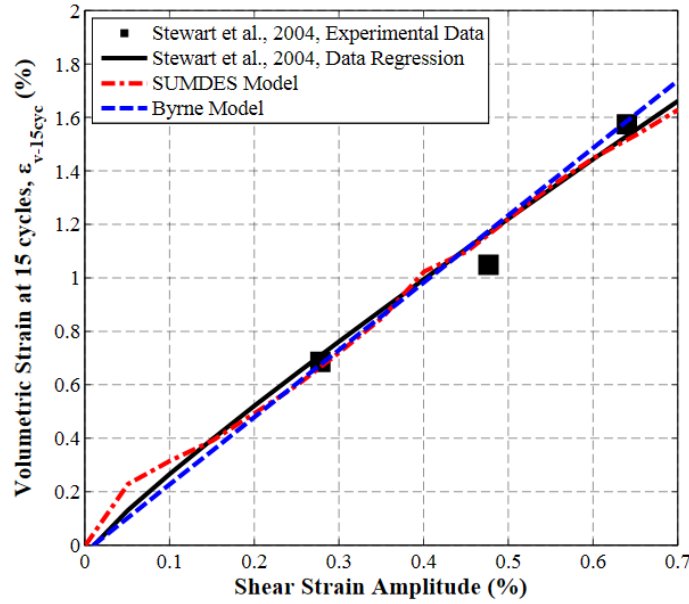


Figure 3. Model predictions and Stewart et al. (2004) test data

### Volumetric Strain Model & Equivalent Number of Cycles – Multi-directional Loading

A limitation of the R-N fatigue theory, and hence a limitation of the Byrne model, is that it was developed for one-dimensional (1D) loading. However, both horizontal components of earthquake shaking contribute to the breakdown of the soil skeleton and commensurate triggering of liquefaction. In previous studies, the multi-directional loading commonly has been accounted for subsequent to the computation of  $n_{eq}$ , e.g., increasing the estimated volumetric strain caused by  $n_{eq}$  cycles of loading (Pyke et al., 1975) or reducing the cyclic resistance required to trigger liquefaction in  $n_{eq}$  cycles of 1D loading (e.g., Seed et al., 1975b). This approach is better suited for situations where the characteristics of the two horizontal components of motion are similar, or at least do not differ significantly. On the contrary, the fault-normal and fault-parallel components of near-fault motions have very different characteristics, as discussed previously. Accordingly, the authors opted to extend the R-N fatigue theory to 2D using numerical element tests, where the volumetric strain response of a finite element subjected to the 2D motions was defined by the reduced-order bounding-surface hypoplasticity constitutive model proposed by Li et al. (1992). The numerical element tests were performed using the utility program, TESTMODL, that is part of the multi-directional site response finite element code SUMDES (Li et al., 1992).

#### TESTMODL

The reduced-order bounding-surface hypoplasticity constitutive model proposed by Li et al. (1992) is built into TESTMODL and can be used to predict the non-linear, inelastic behavior of a soil specimen under a variety of multi-directional loading conditions. TESTMODL can apply the general six component loading paths (three normal and three shear), where loads can be either stress- or strain-controlled, and the soil element can be modeled as either drained or un-drained. Following the



coordinate convention shown in Figure 4, a single horizontal component of motion (e.g., fault-normal or fault-parallel) can be applied at either  $\sigma_{13}$  or  $\sigma_{23}$  as a shear strain-time history to compute the vertical strain in the \*33 direction. To simulate a horizontal soil profile of infinite lateral extent, strains in the \*11 and \*22 directions can be forced to be zero. Thus, the vertical strain in the \*33 direction is equal to the volumetric strain in the element. The volumetric strain in the soil element resulting from being subjected to a set of motions individually in the \*13 or \*23 direction, not simultaneously, are referred to herein as  $(\epsilon_{v,1D-X})_{TESTMODL}$  and  $(\epsilon_{v,1D-Y})_{TESTMODL}$ , while the volumetric strain resulting from the simultaneous application of a set of fault-normal and fault-parallel motions in the \*13 and \*23 directions are denoted as  $(\epsilon_{v,2D})_{TESTMODL}$ .

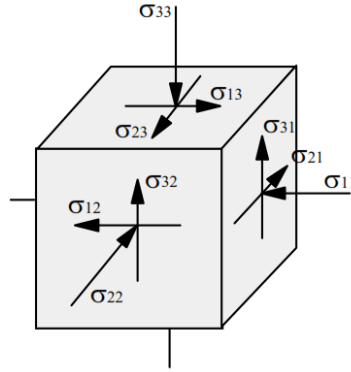


**Figure 4. TESTMODL Coordinate Convention**

#### Model Calibration

The reduced-order bounding-surface hypoplasticity constitutive model in TESTMODL was calibrated using the shear modulus and damping degradation curves proposed by Ishibashi and Zhang (1993) in conjunction with the seismic compression data mentioned above (Stewart et al., 2004). Figure 3 shows a comparison between the TESTMODL model predictions and  $(\epsilon_v)_{\sigma'_{v,z,ref}}$ .

#### $n_{eq}$ for Multi-directional Loading

As stated above, TESTMODL was used to compute the volumetric strains induced in a soil element subjected to the fault-normal and fault-parallel components of motion, individually and simultaneously, resulting in  $(\epsilon_{v,1D-X})_{TESTMODL}$ ,  $(\epsilon_{v,1D-Y})_{TESTMODL}$ , and  $(\epsilon_{v,2D})_{TESTMODL}$  for each set of near-fault motions. To ensure consistency with previous studies that used the Byrne (1991) model to compute  $n_{eq}$  for 1D loading (e.g., Green and Lee, 2006; Lee, 2009), the following relation was used to obtain volumetric strains for computing the number of equivalent cycles for 2D loading ( $n_{eq,2D}$ ):

$$\epsilon_{v,2D} = \left[ \frac{(\epsilon_{v,2D})_{TESTMODL}}{(\epsilon_{v,1D-X})_{TESTMODL} + (\epsilon_{v,1D-Y})_{TESTMODL}} \right] \times \left[ (\epsilon_{v,1D-X})_{Byrne} + (\epsilon_{v,1D-Y})_{Byrne} \right] \quad (8)$$

where:  $(\epsilon_{v,1D-X})_{Byrne}$  and  $(\epsilon_{v,1D-Y})_{Byrne}$  are volumetric strains computed using the Byrne model for the fault-normal and fault-parallel components of motion individually, not simultaneously.

The Byrne model was used to compute  $n_{eq,2D}$ , which is the number of cycles of a 1D sinusoidal load required to induce  $\epsilon_{v,2D}$  in the soil, where the amplitude of the sinusoidal load ( $\gamma_{eff}$ ) was 0.65 times the geometric mean of the peak shear strains in the fault-normal and fault-parallel motions (i.e.,  $\gamma_{max,X}$  and  $\gamma_{max,Y}$ ):

$$\gamma_{eff} = 0.65 \sqrt{\gamma_{max,X} \cdot \gamma_{max,Y}} \quad (9)$$

Figure 5 shows the resulting number of equivalent cycles for the fault-parallel and fault-normal components of motion computed individually ( $n_{eq,1D}$ ) and simultaneously ( $n_{eq,2D}$ ). Also shown in this figure is the number of equivalent cycles correlation developed by Seed et al. (1975a), wherein the motions (non near-fault) were treated individually.

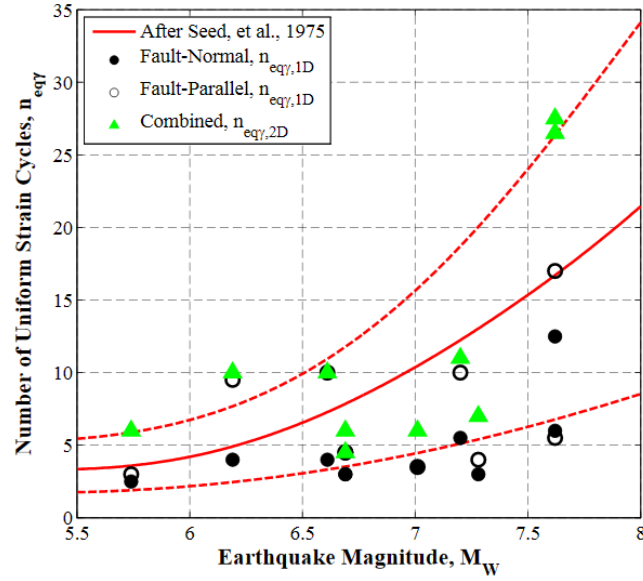


**Figure 5. Number of Equivalent Strain Cycles for Near-Fault 1D and 2D Loading Conditions**

From Figure 5, it can be seen the fault-parallel component tends to yield a greater  $n_{eq,1D}$  than its respective fault-normal counterpart. As  $n_{eq}$  and significant duration of a motion are related (e.g., Green and Terri, 2005), this phenomenon can be explained by the relationship between duration and rupture directivity noted in previous studies (e.g., Somerville et al., 1997; Green et al., 2008). That is, due to the way the near-fault effects manifest in the ground motions, the fault-normal component tends to have a shorter significant duration than the fault-parallel component.

Also from Figure 5, it may be observed that the  $n_{eq,1D}$  values for this study plot below the mean of the Seed et al. (1975a) regression. This is likely due to the site-to-source distances of the motions used in the two studies. Seed et al. (1975a) used non near-fault motions (i.e., motions that are further from the fault rupture), while the study presented herein is focusing on near-fault motions. As shown in Lee (2009), the number of equivalent cycles tends to increase with increased site-to-source distance. Finally, as expected, the  $n_{eq,2D}$  values are generally greater than the  $n_{eq,1D}$  values, with the average ratio of  $n_{eq,2D}/n_{eq,1D}$  for the fault-normal and fault-parallel components being 2.4 and 1.8, respectively.

### MAGNITUDE SCALING FACTORS FOR MULTI-DIMENSIONAL SHAKING

To assess the influence of near-fault motions on liquefaction triggering,  $n_{eq,2D}$  values were used to compute MSF for the motions. As shown in Idriss (1997) and Green (2001),  $n_{eq}$  and MSF are related by:

$$MSF = \left( \frac{n_{eq,M7.5}}{n_{eq}} \right)^m \quad (10)$$

where  $n_{eq,M7.5}$  is the number of cycles for a reference earthquake magnitude of 7.5, traditionally taken as 15 cycles (Seed and Idriss, 1982), and  $m$  is the negative of the slope of a log-log plot of cyclic stress ratio (CSR) versus number of cycles to liquefaction for a soil having a given relative density and confined at a given effective stress. For the study presented herein,  $m$  was set equal to 0.35, which is falls within the range of published values and is approximately equal to that determine by Yoshimi et al. (1984) from cyclic triaxial tests performed on high-quality, undisturbed samples obtained by frozen sampling.

As mentioned above,  $n_{eq,M7.5}$  is traditionally assumed to be 15 cycles. However, this value is for 1D loading (i.e.,  $n_{eq,M7.5,1D}$ ). Accordingly, the approach outlined above to compute  $n_{eq,2D}$  for near-fault motions was applied to sets of horizontal components of non near-fault rock motions ( $V_s > 600$  m/s)



recorded during earthquakes having  $M_w 7.5 \pm 0.3$  and site-to-source distances less than 80 km. In total 15 sets of motions were used to compute  $n_{eq,M7.5\_2D}$ , all of them coming from the NGA 1 database, with the average  $n_{eq,M7.5\_2D}$  equal to 24.9.

The resulting near-fault MSF that accounts for the contributions of both the fault-normal and fault-parallel components of motions (i.e.,  $MSF_{2D}$ ) is plotted in Figure 6. For reference,  $MSF_{2D}$  for non near-fault motions computed using the approach outlined in this study is also shown in this figure, as is the range of MSF recommended by Youd et al. (2001). As may be observed from this figure, the near-fault  $MSF_{2D}$  are generally higher than the non near-fault  $MSF_{2D}$  and the MSF recommended by Youd et al. (2001), implying that near-fault motions are less demanding, from a liquefaction triggering perspective, than non near-fault motions having an equal amplitudes. This may be one of several factors that resulted in less severe liquefaction occurring during the Darfield earthquake than the Christchurch earthquake (Figure 1).

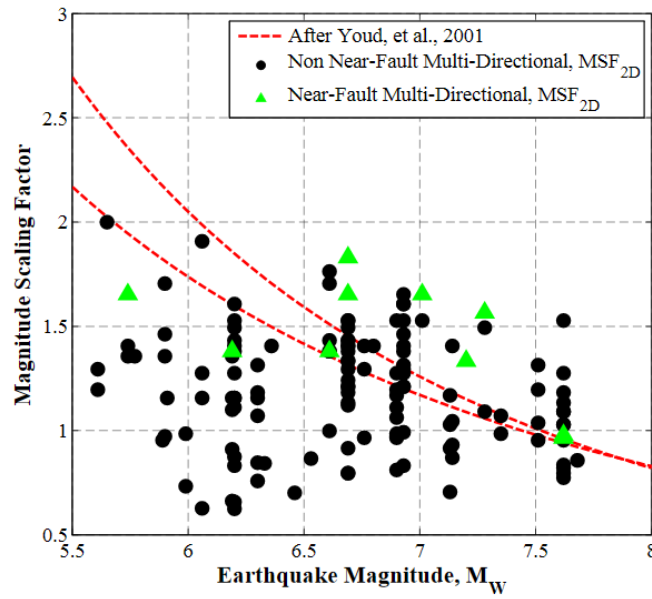


**Figure 6. Magnitude Scaling Factor for Near-Fault and Non Near-Fault for 2D Loading**

## CONCLUSION

Based on the analysis of the ten fault-normal and fault parallel near-fault ground motion sets, the influence of rupture (forward) directivity on liquefaction triggering was evaluated. Using a 1D variant of the R-N fatigue theory wherein volumetric strain was used as the damage metric, it was determined that the fault-normal components of motion (i.e. motions containing a pronounced velocity pulse) resulted in a lower number of uniform strain cycles than the fault-parallel counterpart. This finding is consistent with that of Green et al. (2008) who used a low cycle variant of the P-M fatigue theory to analyze near fault motions. To determine the combined influence of both the fault-normal and fault-parallel components, a 2D variant of the R-N fatigue theory was developed as part of this study, wherein volumetric strain was again used as the damage metric. To assess the influence on liquefaction triggering, MSF were computed for the combined near-fault components of motions and compared with ones developed for non near-fault motions that are commonly used in practice. The near-fault MSF were generally higher than both the non near-fault MSF commonly used in practice, implying that near-fault motions are less demanding, from a liquefaction triggering perspective, than non near-fault motions. This may be one of several factors that resulted in less severe liquefaction occurring during the Darfield earthquake than the Christchurch earthquake.

## ACKNOWLEDGEMENTS

Primary support for the US authors was provided by the U.S. National Science Foundation (NSF) grants CMMI-1030564 and CMMI-1306261 and an NSF EAPSI Fellowship awarded to L. Carter. However, any opinions, findings, and conclusions or recommendations expressed in this material are those of the authors and do not necessarily reflect the views of the National Science Foundation.

## REFERENCES

- Alavi, B. and Krawinkler, H. (2001). "Effects of Near-Fault Ground Motions on Framed Structures," Blume Center Report 138, Stanford, CA, USA.
- Andrus, R.D., Piratheepan, P., Ellis, B.S., Zhang, J., and Juang, C.H. (2004). "Comparing liquefaction evaluation methods using penetration-Vs relationships," *Soil Dynamics and Earthquake Engineering*, 24(9-10), 713-721.
- Annaki, M. and Lee, K.L. (1977). "Equivalent Uniform Cycle Concept for Soil Dynamics," *Journal of the Geotechnical Engineering Division*, ASCE, 103(GT6), 549-564.
- Bradley, B.A. (2012a). "Strong ground motion characteristics observed in the 4 September 2010 Darfield, New Zealand earthquake," *Soil Dynamics and Earthquake Engineering*, 42, 32-46.
- Bradley, B.A. (2012b). "Observed Ground Motions in the 4 September 2010 Darfield and 22 February 2011 Christchurch Earthquakes," *Proc. 2012 New Zealand Society of Earthquake Engineering Conference (2012 NZSEE)*, 13-15 April 2012, Christchurch, New Zealand, Paper No. 037.
- Bradley, B.A. and Cubrinovski, M. (2011). "Near-Source Strong Ground Motions Observed in the 22 February 2011 Christchurch Earthquake," *Bulletin of the New Zealand Society for Earthquake Engineering*, 44(4), 181-194.
- Byrne, P.M. (1991). "A cyclic shear-volume coupling and pore pressure model for sand," *Proc. 2nd International Conference on Recent Advances in Geotechnical Earthquake Engineering and Soil Dynamics*, Paper No. 1.24, St. Louis, Missouri.
- Cetin, K.O. (2000). "Reliability-Based Assessment of Seismic Soil Liquefaction Initiation Hazard," *PhD. Dissertation*. Department of Civil Engineering, University of California, Berkeley.
- Duku, P.M., Stewart, J.P., Whang, D.H., and Yee, E. (2008). "Volumetric strains of clean sands subject to cyclic loads," *Journal of Geotechnical and Geoenvironmental Engineering*, ASCE, 134(8), 1073-1085.
- Green, R.A. (2001). "Energy-Based Evaluation and Remediation of Liquefiable Soils," *Ph.D. Dissertation* (J.K. Mitchell, Advisor), Department of Civil and Environmental Engineering, Virginia Polytechnic Institute and State University (Virginia Tech), Blacksburg, VA, 397pp. <http://scholar.lib.vt.edu/theses/available/etd-08132001-170900/>
- Green, R.A. and Lee, J. (2006). "Computation of Number of Equivalent Strain Cycles: A Theoretical Framework," *Geomechanics II: Testing, Modeling, and Simulation* (P.V. Lade and T. Nakai, eds.), ASCE Geotechnical Special Publication 156, 471-487.
- Green, R.A., Lee, J., White, T.M., and Baker, J.W. (2008). "The significance of near-fault effects on liquefaction," *Proc. 14<sup>th</sup> World Conference on Earthquake Engineering*, Beijing, China.
- Green, R.A. and Terri, G.A. (2005). "Number of Equivalent Cycles Concept for Liquefaction Evaluations—Revisited," *Journal of Geotechnical and Geoenvironmental Engineering*, ASCE, 131(4), 477-488.
- Hall, J.F., Heaton, T.H., Halling, M.W., and Wald, D.J. (1995). "Near-Source Ground Motions and Its Effects on Flexible Buildings," *Earthquake Spectra*, 11(4), 569-605.
- Idriss, I.M. (1997). "Evaluation of Liquefaction Potential and Consequences: Historical Perspective and Updated Procedures," Presentation Notes: 3<sup>rd</sup> Short Course on Evaluation and Mitigation of Earthquake Induced Liquefaction Hazards, 13-14 March 1997, San Francisco, CA, 16pp.
- Ishibashi, I. and Zhang, X. (1993). "Unified dynamic shear moduli and damping ratios of sand and clay". *Soils and Foundations*, 33(1), 182-191.
- Ishihara, K. and Nagase, H. (1988). "Multi-directional irregular loading tests on sand," *Soil Dynamics and Earthquake Engineering*, 7(4), 201-212.
- Ishihara, K. and Yasuda, S. (1973). "Sand Liquefaction Under Random Earthquake Loading Condition," *Proc. 5<sup>th</sup> World Conference on Earthquake Engineering*, Rome, Italy, 1, 329-338.
- Joshi, V.A., Bradley, B.A. (2013), "Empirical Analysis of Near-Fault Forward-Directivity Effects in the 2010-11 Canterbury Earthquakes," *Proc. 2012 New Zealand Society of Earthquake Engineering Conference (2013 NZSEE)*, 26-28 April 2013, Wellington, New Zealand.
- Lee, J., (2009), "Engineering Characterization of Earthquake Ground Motions." *PhD. Dissertation*. Department of Civil Engineering, University of Michigan.

- Li, X.S., Wang,Z.L., and Shen, C.K.(1992). "SUMDES: A Nonlinear Procedure for Response Analysis of Horizontally-layered Sites Subjected to Multi-directional Earthquake Loading," Department of Civil Engineering, University of California, Davis, 88p.
- Liu, A.H., Stewart, J.P., Abrahamson, N.A., and Moriawaki, Y. (2001). "Equivalent Number of Uniform Stress Cycles for Soil Liquefaction Analysis," *Journal of Geotechnical and Geoenvironmental Engineering*, ASCE, 127(12), 1017-1026.
- Luco, N. and Cornell, C.A. (2007). "Structure-Specific Scalar Intensity Measures for Near-Source and Ordinary Earthquake Ground Motions," *Earthquake Spectra*, 23(2), 357-392.
- Martin, G.R., Finn, W.D.L., and Seed, H.B. (1975). "Fundamentals of liquefaction under cyclic loading," *Journal of the Geotechnical Engineering Division*, ASCE, 101(GT5), 423-438.
- Miner, M.A. (1945). "Cumulative Damage in Fatigue," *Transactions*, ASME, 67, A159-A164.
- Palmgren, A. (1924). "Die Lebensdauer Von Kugella Geru." *ZVDI*, 68(14), 339-341.
- Pyke, R., Seed, H.B., and Chan, C.K. (1975). "Settlement of Sands Under Multidirectional Shaking," *Journal of the Geotechnical Engineering Division*, ASCE, 101(GT4), 379-398.
- Richart, F.E. and Newmark, N.M. (1948). "An Hypothesis for Determination of Cumulative Damage in Fatigue," *ASTM Proceedings*, 48, 767-800.
- Seed, H.B., Idriss, I.M., Makdisi, F., and Banerjee, N. (1975a). "Representation of Irregular Stress Time Histories by Equivalent Uniform Stress Series in Liquefaction Analysis," Report No. EERC 75-29, Earthquake Engineering Research Center, College of Engineering, Univ. of California, Berkeley, California, United States.
- Seed, H.B., Lee, K.L., Idriss, I.M., and Makdisi, F.I. (1975b). "The Slides in the San Fernando Dams during the Earthquake of February 9, 1971," *Journal of the Geotechnical Engineering Division*, ASCE, 101(GT7), 651-688.
- Seed, H.B. and Idriss, I.M. (1982). "Ground Motions and Soil Liquefaction During Earthquakes," Earthquake Engineering Research Institute, Oakland, CA, USA.
- Shahi, S., Baker, J., (2012). November 1<sup>st</sup>, 2012 Pulse Classifications form NGA West2 database, Stanford University, California, [http://www.stanford.edu/~bakerjw/pulse\\_classification\\_v2/Pulse-like-records.html](http://www.stanford.edu/~bakerjw/pulse_classification_v2/Pulse-like-records.html)
- Somerville, P.G., Smith, N.F., Graves, R.W., and Abrahamson, N.A. (1997). "Modification of Empirical Strong Ground Motion Attenuation Relations to Include the Amplitude and Duration Effects of Rupture Directivity," *Seismological Research Letters*, 68(1), 199-222.
- Stewart, J.P., Whang, D.H., Moyneur, M., and Duku, P.M. (2004), "Seismic Compression of As-Compacted Fill Soils with Variable Levels of Fines Content and Fines Plasticity," *Earthquake Damage Assessment and Repair Project*, CUREE
- Tokimatsu, K., and Seed, H.B. (1987). "Evaluation of settlement in sands due to earthquake shaking," *Journal of Geotechnical Engineering*, ASCE, 113(8), 861-878.
- Wer-Asturias, R. (1982). "The equivalent number of cycles of recorded accelerograms for soil liquefaction studies," MS thesis, Rensselaer Polytechnic Institute, Troy, N.Y.
- Yoshimi, Y., Tokimatsu, K., Kaneko, O., and Makihara, Y. (1984). "Undrained Cyclis Shear Strength of a Dense Niigata Sand," *Soils and Foundations*, 24(4), 131-145.
- Youd, T.L., Idriss, I.M., Andrus, R.D., Arango, I., Castro, G., Christian, J.T., Dobry, R. Finn, W.D.L., Harder, L.F., Hynes, M.E., Ishihara, K., Koester, J.P., Liao, S.S.C., Marcuson III, W.F., Martin, G.R., Mitchell, J.K., Moriawaki, Y., Power, M.S., Robertson, P.K., Seed, R.B., and Stokoe II, K.H. (2001). "Liquefaction Resistance of Soils: Summary Report from the 1996 NCEER and 1998 NCEER/NSF Workshops on Evaluation of Liquefaction Resistance of Soils," *Journal of Geotechnical and Geoenvironmental Engineering*, ASCE, 127(4), 297-313